THE ASTROPHYSICAL JOURNAL, 395:L29–L32, 1992 August 10

ASTRO-1 ULTRAVIOLET IMAGING OF THE 30 DORADUS AND SN 1987A FIELDS WITH THE ULTRAVIOLET IMAGING TELESCOPE

KWANG-PING CHENG,[1,2,3] ANDREW G. MICHALITSIANOS,[1] PAUL HINTZEN,[1,3,4] RALPH C. BOHLIN,[5]
ROBERT W. O'CONNELL,[6] ROBERT H. CORNETT,[7] MORTON S. ROBERTS,[8] ANDREW M. SMITH,[1]
ERIC P. SMITH,[1] AND THEODORE P. STECHER[1]

Received 1992 March 31; accepted 1992 May 26

ABSTRACT

During the *Astro-1* mission, near- and far-UV images of selected fields in the Magellanic Clouds were obtained using the Ultraviolet Imaging Telescope (UIT). These ultraviolet images, centered on SN 1987A, 30 Doradus, supernova remnants N49A + B, and SMC-A, provide the first wide-field (40′ in diameter), high spatial resolution (2″–3″) UV images of these regions. The 30 Doradus data reveal a rich field of luminous UV-bright stars, clusters, and associations: within the 3′ diameter central cluster, there are 181 stars brighter than $m_{2558} = 16.5$, and 197 stars brighter than $m_{1615} = 16.4$. We have derived UV fluxes from the 30 Doradus central cluster and from its UV-bright core, R136. A region within 5″ of R136 produces ∼14% of the far-UV flux ($\lambda = 1892$ Å) and ∼16% of the near-UV flux ($\lambda = 2558$ Å) emitted from the 3′ diameter central cluster. The derived UV luminosity of R136 at 1892 Å is only 7.8 times that of the nearby O6–O7 Iaf star, R139, and the $m_{1892} - m_V$ colors of R136 are similar to other O or Wolf-Rayet stars in the same region. The UIT data, combined with published observations at longer wavelengths, indicate that there is no observational evidence for a supermassive star in R136. In the UIT images, we also detect an extensive dust feature, which extends throughout the 30 Doradus and SN 1987A fields. Diffuse UV emission at low flux levels runs from northeast to southwest at the northern boundary of N157A, N157B, and N157C, corresponding closely to the extended infrared emission seen in the *IRAS* 60 μm high-resolution (HiRes) image. The observed correlation between the UV and the IR emission suggests that the dust scatters a substantial fraction of the incident UV photons, while absorbing some of the remainder and reemitting this energy in the IR. We have compared the UIT images with the *Einstein* X-ray images, *IRAS* HiRes images, and ground-based CCD fields in [O III] λ5007, Hα, *B*, *R*, *U*, and Strömgren *u*. This comparison is extremely useful in identifying and studying large H II regions, stellar windblown cavities, and extended large-scale filaments which are delineated largely by the expansion of supernova shells.

Subject headings: dust, extinction — H II regions — ISM: bubbles — Magellanic Clouds — stars: fundamental parameters — supernova remnants — ultraviolet: general

1. INTRODUCTION

During the *Astro-1* mission, ultraviolet images of selected fields in the Large Magellanic Cloud (LMC) were obtained using the Ultraviolet Imaging Telescope (UIT) with an assortment of broad and narrow filters which cover the near-UV and far-UV (2000–3500 Å and 1200–2000 Å, respectively). Each UIT image covers a 40″ diameter field of view (∼200 *HST* Wide Field Camera fields) with spatial resolution of 2″–3″.

The LMC is a unique laboratory for investigating galactic structure and the physics of star formation. In the LMC the supernova remnants (SNRs) are important because they reflect the characteristic shape of the star formation front. The UIT produced the first high-quality ultraviolet imagery of the SNRs in the LMC, since lines of C III] λ1909, He II λ1640, and C IV λ1550 emanating from a diffuse continuum can be sampled with the available far-UV filters. There are 32 known SNRs in the LMC (Forest, Spenny, & Johnson 1988), and five are in the UIT 30 Doradus (SK −69 239) and SN 1987A fields.

A comparison of the UIT LMC images with X-ray (*Einstein*), optical (CCD), and infrared (*IRAS*) images is extremely useful in identifying and studying luminous hot stars and OB associations, giant H II regions, clusters of massive stars still embedded in dust, the large-scale distribution of ionized gas and dust, the correlation between Hα emission and UV morphology, and the structure of the coronal component of the interstellar medium (ISM).

2. OBSERVATIONS

2.1. *UV (UIT) Images*

The UIT optics and detectors are described in detail by Stecher et al. (1992). Images were recorded on II-aO film behind a two-stage UV-sensitive image tube and digitized with a PDS microdensitometer. All the UIT data analysis has been done using the UIT image processing system. The resulting 2048 × 2048 images, at 1.″14 pixel^{-1}, have been calibrated and flat-fielded.

In Table 1 we list all the Large Magellanic Cloud images obtained with the UIT in 1990 December using six broad-band

[1] Laboratory for Astronomy and Solar Physics, NASA/GSFC, Greenbelt, MD 20771.
[2] National Research Council Postdoctoral Fellow.
[3] Visiting Astronomers at the Cerro Tololo Inter-American Observatory of the NOAO operated by AURA, Inc., under contract to the NSF.
[4] Department of Physics and Astronomy, University of Nevada, Las Vegas, NV 89154.
[5] Space Telescope Science Institute, Baltimore, MD 21218.
[6] Astronomy Department, University of Virginia, Charlottesville, VA 22903.
[7] Hughes STX Corporation, 4400 Forbes Boulevard, Lanham, MD 20706.
[8] National Radio Astronomy Observatory, Edgemont Road, Charlottesville, VA 22903.

TABLE 1

LMC UIT IMAGES

UIT FIELDS (40′ diameter)	FIELD CENTER R.A.(1950)	FIELD CENTER Decl.(1950)	FILTER (λ_0/FWHM)	EXPOSURES (s)
30 Doradus (SK −69 239)	$05^h39^m09^s.9$	−69°07′07″	B5 (1615/225)	473,* 69.5, 17.4*
			A2 (1892/412)	112, 22.8,* 4.02*
			A4 (2205/244)	112, 22, 4.13
			A5 (2558/456)	472,* 112, 22.2, 18.3,* 4.01*
SN 1987A	05 35 55.5	−69 16 58	B1 (1521/354)	159
			B5 (1615/225)	1270, 225, 140, 50.6, 27.7
			A5 (2558/456)	235, 8.85
N49A+B	05 25 59.5	−66 07 41	B5 (1615/225)	222, 44.8, 8.34
			A3 (1964/173)	44, 9.2, 1.28

NOTE.—Asterisks following exposure times identify UIT images used in this study.

near- and far-UV filters. Most of the UIT pointings in the LMC were centered on 30 Doradus, the largest H II region in the Local Group, and on SN 1987A. The UIT images used in the present study are identified with asterisks in Table 1.

2.2. *Ground-based Images*

Complementary ground-based images of the 30 Doradus and SN 1987A fields were obtained in 1992 February with a Tek 2048 CCD on the Cerro Tololo Inter-American Observatory (CTIO) 36 inch (0.9 m) telescope. Each ground-based image represents a mosaic of four 2048 × 2048 CCD subimages yielding a total field of view of 30′ × 30′, comparable to that of the UIT images. With a 0.″445 pixel^{-1} plate scale and 2″ seeing, the resolution of our ground-based images closely matches the UIT resolution. For each subimage in each filter (*B*, *R*, Hα, *U*, Strömgren *u*, and [O III] λ5007), three exposures were obtained and median-filtered to remove radiation events. A summary of the ground-based data is presented in Table 2.

3. ANALYSIS

Our preliminary analysis of the UIT data concentrates on the 30 Doradus (SK −69 239) region; a summary of the structures involved and the nomenclature we adopt is provided in Table 3. These UV images of the 30 Doradus region enable us to map the filamentary nebular boundaries formed by supernova shocks and radiatively driven, high-velocity winds from luminous O and B supergiants. Figure 1 (Plate L13) shows the UIT B5 image (λ1615 Å) of the 30 Doradus region overlaid with contours from the *Einstein* Imaging Proportional Counter (IPC) soft X-ray data (0.16–3.5 keV, 3″ resolution). The soft X-ray image reveals the presence of hot gas contained in cavities formed either by stellar winds or by supernova shocks (Wang & Helfand 1991). The UV-bright core of the 30 Doradus nebula, the cluster 7157A (NGC 2070), is a bright, diffuse X-ray emitter with a total luminosity of 2×10^{37} ergs s^{-1} in the 0.16–3.5 keV band (flux-integrated within 12′ radius). Also bright in the UV is LH 99, the central OB association in N157B, a Crab-like supernova remnant and strong X-ray source located at the southwestern corner of the 30 Doradus nebula.

3.1. *Discrete UV Sources*

The 30 Doradus central cluster, N157A, is characterized by numerous O stars, B supergiants, and Wolf-Rayet stars (Melnick 1985). Many faint discrete sources are seen in the UIT images. Hill et al. (private communication) have identified 181 stars brighter than $m_{2558} = 16.9$ in the A5 images, and 197 stars brighter than $m_{1615} = 16.4$ in the B5 images within the 3′ diameter field encompassing the central cluster (Fig. 2, *large circle*). We find that R136, the brightest component of N157A at visible wavelengths, is also the brightest component in the UV (see Fig. 2 [Pl. L14], where R136 is indicated by the smaller circle). Our examination of data in the *IUE* archives indicates that R136 is larger than a point source but smaller than the 10″ × 20″ *IUE* large aperture. In this study we have used the conventions for the size of R136 suggested by Seggewiss (1984), who adopts a diameter of 7″, and by Walborn (1991), who uses

TABLE 2

LMC GROUND-BASED IMAGES:[a] 30 DORADUS (SK −69 239) AND SN 1987A

Filter (λ_0/FWHM)	Total Exposure Time (s)
Hα (6565/50)	1800
[O III] (5007/50)	1800
Strömgren *u* (3515/300)	900
U	1800
B	360
R	360

[a] A 30′ × 30′ mosaic was produced for each passband by combining four Tek 2048 CCD images (0.″445 pixel^{-1}).

TABLE 3

CHARACTERISTIC DIMENSIONS[a]

Region	Linear Size	Angular Diameter[b]
LMC	5 kpc	5°
30 Doradus region	1 kpc	1°
30 Doradus nebulae	200 pc	15′
N157A (central cluster in 30 Doradus)	40 pc	3′
R136 (UV bright core of N157A)	2–2.5 pc	7″–10″[c]
R136a (brightest component of R136)	0.25 pc	1″

[a] The conventions suggested by Walborn 1991.
[b] The distance to the LMC was assumed to be 52.5 kpc.
[c] Seggewiss 1984 used a diameter of 7″ for R136; Walborn 1991 chose 10″.

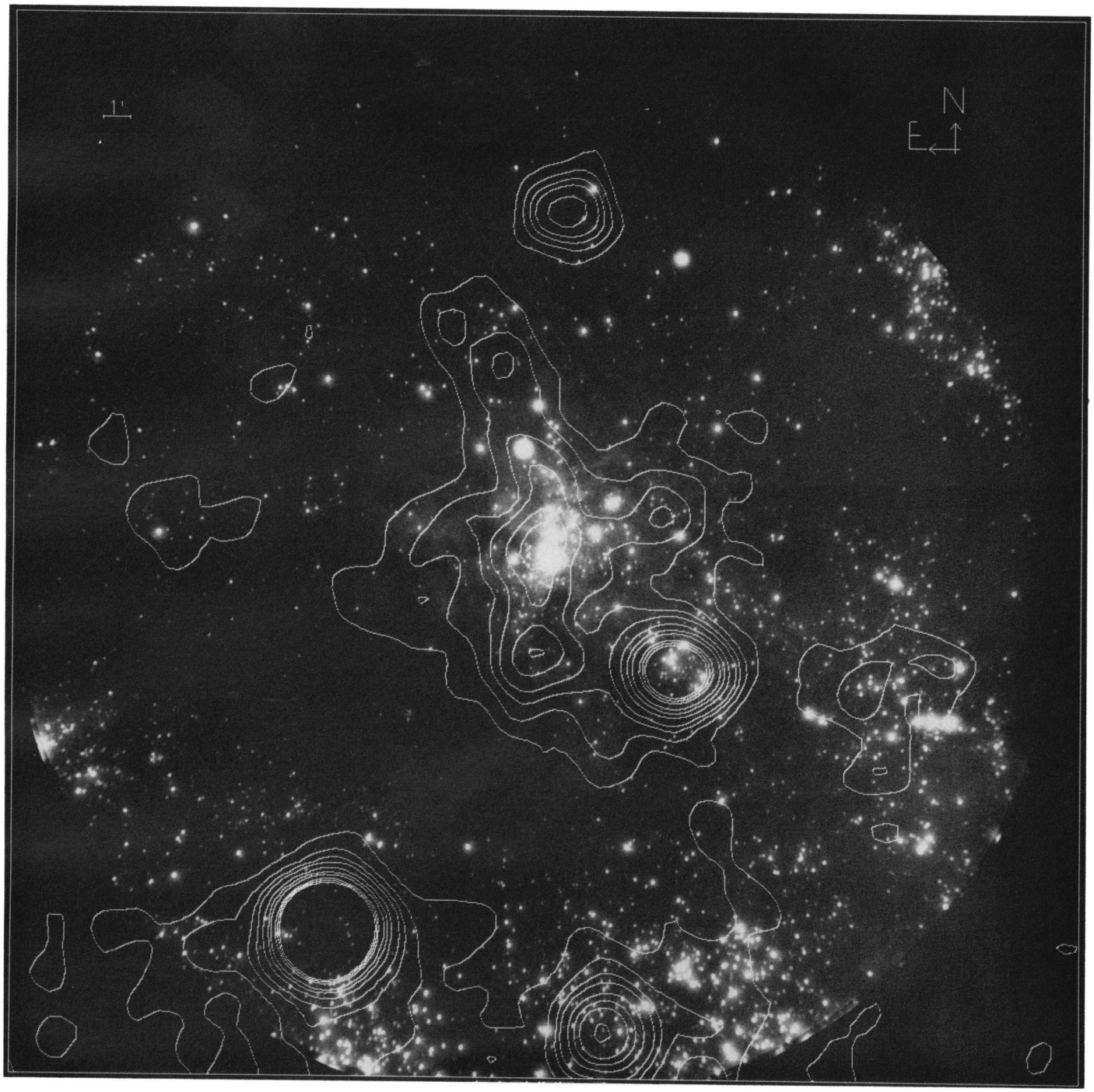

FIG. 1.—UIT far-UV image of the 30 Doradus field (40′ in diameter, $\lambda_0 = 1615$ Å, FWHM = 225 Å, exposure time = 473 s) with the *Einstein* IPC X-ray contours overlaid.

CHENG et al. (see 395, L30)

PLATE L14

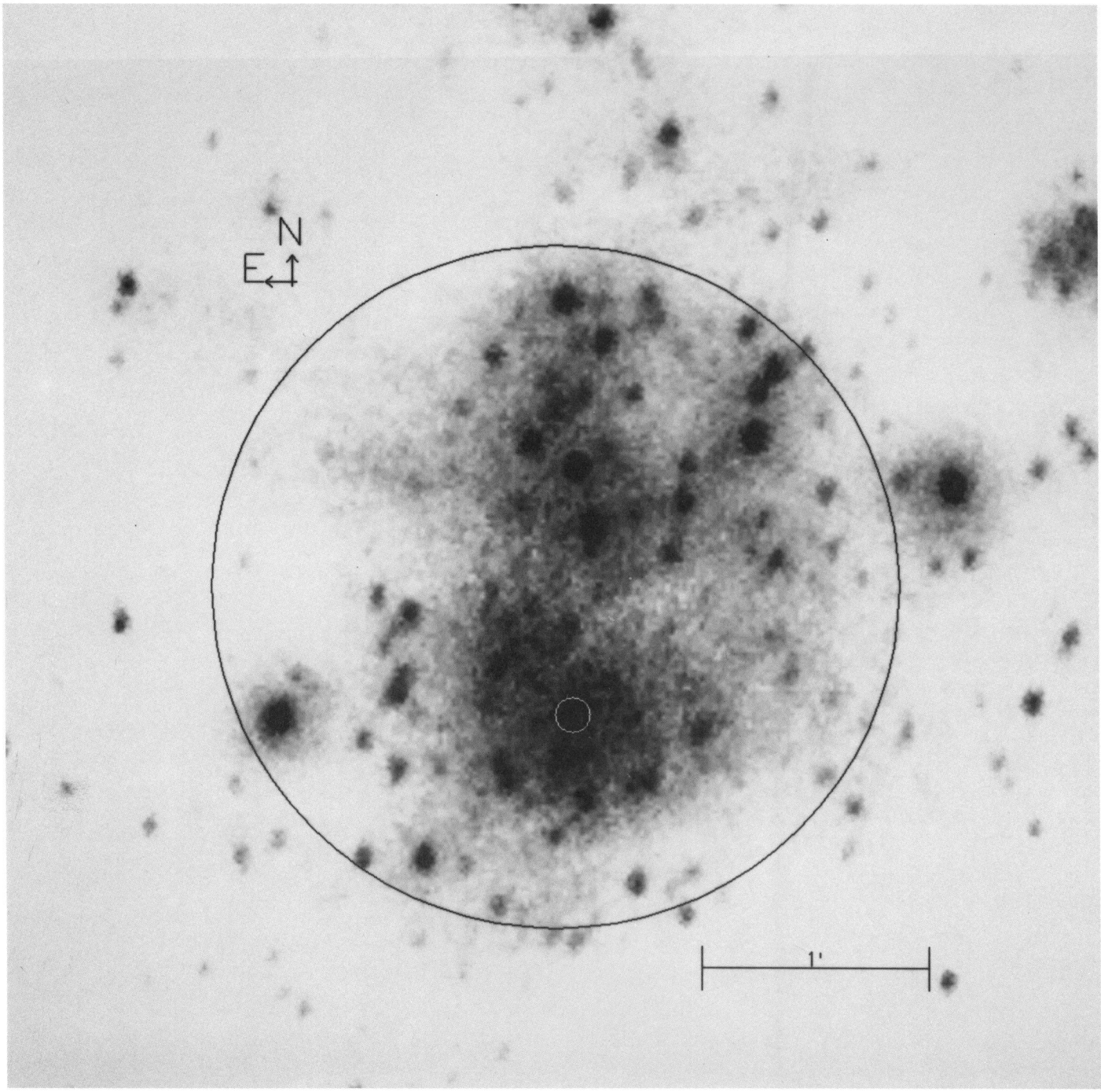

FIG. 2.—Central field of the UIT far-UV 30 Doradus image (B5, λ_0 = 1615 Å, FWHM = 225 Å, exposure time = 17.4 s). The large circle has a diameter of 3′, and the small circle centered on the UV-bright core R136 has a radius of 5″.

CHENG et al. (see 395, L30)

a diameter of about 10″. Moffat, Seggewiss, & Shara (1985) have derived an approximate luminosity ratio, L_{UV}(R136, 10″ diameter)/L_{UV}(30 Doradus cluster, 2′ diameter) ≈ 17%, from *IUE* slit spectroscopy published by Koornneef & Mathis (1981). However, the diameter of the UV-emitting region associated with the 30 Doradus cluster is roughly 3′, significantly larger than that inferred from the mapping performed with the *IUE* large aperture. The UIT 40′ diameter images therefore provide greatly improved UV fluxes for both R136 and the 30 Doradus central cluster as a whole. Photometry was obtained from the digitized UIT images by summing the pixels contained in the chosen circular aperture, subtracting an appropriate sky value, and applying zero-point corrections determined for each aperture. We find that R136 (~10″ in diameter) contributes ~14% at 1892 Å and ~16% at 2558 Å of the total, integrated UV flux emitted by the 3′ diameter central cluster in 30 Doradus (see Fig. 2 and Table 3).

The photometry we derived for R136 and other comparison stars in the same complex (R133, R135, R137, R139, and R145) is presented in Table 4. According to Fitzpatrick's (1985) study of interstellar extinction variations in the 30 Doradus region, the differential extinction among our stars, all located within 1′.5 of the 30 Doradus core, may be ignored to first order. Since we are interested in a relative comparison of blue stars in this region, we have not corrected the magnitudes for reddening, as that would only introduce errors due to the uncertainty in R. We adopt the apparent visual magnitude of R136 from Seggewiss (1984) and the apparent visual magnitudes of other stars from the SIMBAD data base, which also provides the most recent published spectral types.

R136 itself is a complex multiple system which has been resolved into 28 components within a radius of 4″.6 (Walborn 1986). Using speckle imaging, Weigelt & Baier (1985) demonstrated that R136a, the visually brightest component of R136, is a compact cluster of eight stars (R136a1–R136a8) roughly 0″.7 in diameter. This result has been recently confirmed by the *HST* Faint Object Camera (Weigelt et al. 1991), but the physical nature of the brightest component, R136a1, still remains uncertain. Early studies of R136a yielded mass estimates of 500–2500 $M_\odot$ (Schmidt-Kaler 1980; Cassinelli, Mathis, & Savage 1981). After speckle interferometry resolved R136a, Walborn (1986) calculated an upper mass limit of 250 $M_\odot$ for R136a1, the brightest subcomponent of R136a. This is an order of magnitude smaller than the previous estimates for R136a but still considerably larger than the conventional theoretical upper limit on stellar masses, 60–120 $M_\odot$ (Ledoux 1970; Conti & Burnichon 1975). Therefore, the question "Is R136a1 a supermassive star or an unresolved star cluster?" remains unanswered. A supermassive star with mass ~250 $M_\odot$ can be expected to be much more luminous than "normal" stars with M = 60–120 $M_\odot$ (Maeder 1980). Also, Maeder (1980) concludes that such a supermassive star would evolve "directly toward the left in the H-R diagram" as it left the main sequence and therefore might have abnormally blue colors, though an optically thick stellar wind would also have a major effect on colors. However, the derived UV luminosity of R136 at 1892 Å is only 7.8 times that of the nearby O6–O7 Iaf star R139, and the UV colors of R136 are similar to normal O or Wolf-Rayet WN stars. Consequently, the bolometric luminosity and mass of the visually brightest component in R136, R136a1, cannot be substantially greater than those for other luminous O stars in the 30 Doradus complex (see Table 4). There is therefore no observational evidence for a supermassive star in R136.

3.2. *Large-Scale Structures*

We find a good correlation between the Hα morphology and the near-UV continuum morphology of the 30 Doradus region, an ideal region to study the complicated relationship between massive star formation and the structure of the ISM. Based on the UIT images and the Hα mosaic (see Fig. 3 [Pl. L15]), one can investigate the structure of the ISM created by the SNR shocks. Note, for example, the double shock fronts lying ~6′ west of the 30 Doradus center (position A in Fig. 3).

Superbubbles and windblown cavities in this field provide a most effective setting for investigating the general structure of the ISM. Both strong [O III] and Hα emission in galactic H II regions reflect the presence of hot photoionizing O stars. The central cavity may have been swept clear of gas and dust by radiation pressure from the central stars. The ~60 pc large-scale windblown bubble at the southern boundary of the 30 Doradus Nebula is an illustrative example (7′ away from the 30 Doradus center, position B in Fig. 3). It has an almost perfect spherical geometry (see Fig. 4*d* [Pl. L16] the Hα image), which provides an ideal case for bubble modeling. Near-UV emission detected in this region (see Fig. 4*c*, the UIT A5 2558 Å image) arises from both stellar sources and ambient dust (scattered UV light), while the warm gas shell exhibits strong [O III] λ5007 emission as seen in Figure 4*a*. Since the diffuse UV emission does not drop off as rapidly as two-photon emission would at shorter wavelengths, i.e., 1500 Å, one can rule out two-photon emission as an important contributor to the faint

TABLE 4

UV COLORS OF R136 AND OTHER BLUE STARS IN THE SAME REGION

Object	Spectral Type[a]	m_V[a]	m_{2558}	m_{1892}	m_{1615}	$m_{1892}-m_{2558}$	$m_{1892}-m_V$	$m_{1615}-m_{2558}$	$m_{1615}-m_V$
R136 (7″ in diameter)	...	10.0[b]	7.97 ± 0.20	7.65 ± 0.20	7.50 ± 1.00[c]	−0.32	−2.35	−0.47	−2.50
R136 (10″ in diameter)	...	...	7.80 ± 0.20	7.54 ± 0.20	7.40 ± 1.00[c]	−0.26	−2.46	−0.40	−2.60
R133 (HD 269908)	O7–O8	12.47[d]	10.62 ± 0.06	10.07 ± 0.06	10.01 ± 0.05	−0.55	−2.40	−0.61	−2.46
R135	WN7	12.89	11.00 ± 0.08	11.05 ± 0.12	10.90 ± 0.10	0.05	−1.84	−0.10	−1.99
R137	B0.5 Ia	12.00[e]	10.48 ± 0.10	10.34 ± 0.20	10.40 ± 0.10	−0.14	−1.66	−0.08	−1.60
R139	O6–O7 Iaf	11.97	9.81 ± 0.05	9.88 ± 0.05	9.50 ± 0.10	0.07	−2.09	−0.31	−2.47
R145 (HD 269928)	WN6	12.02	11.04 ± 0.06	10.30 ± 0.11	10.09 ± 0.07	−0.74	−1.72	−0.95	−1.93

[a] The spectral types and V-magnitudes listed in this table are generally based on SIMBAD data base, but see the footnotes for R133, R136, and R137.
[b] V ~ 10 for R136 in a diaphragm of 7″ diameter (Seggewiss 1984).
[c] The large rms error reflects the uncertainty due to a bad pixel inside the photometric diaphragm.
[d] For R133 we derive the visual apparent magnitude from Walborn's (1986) absolute magnitude.
[e] For R137 we adopt m_V from Lortet & Testor 1991.

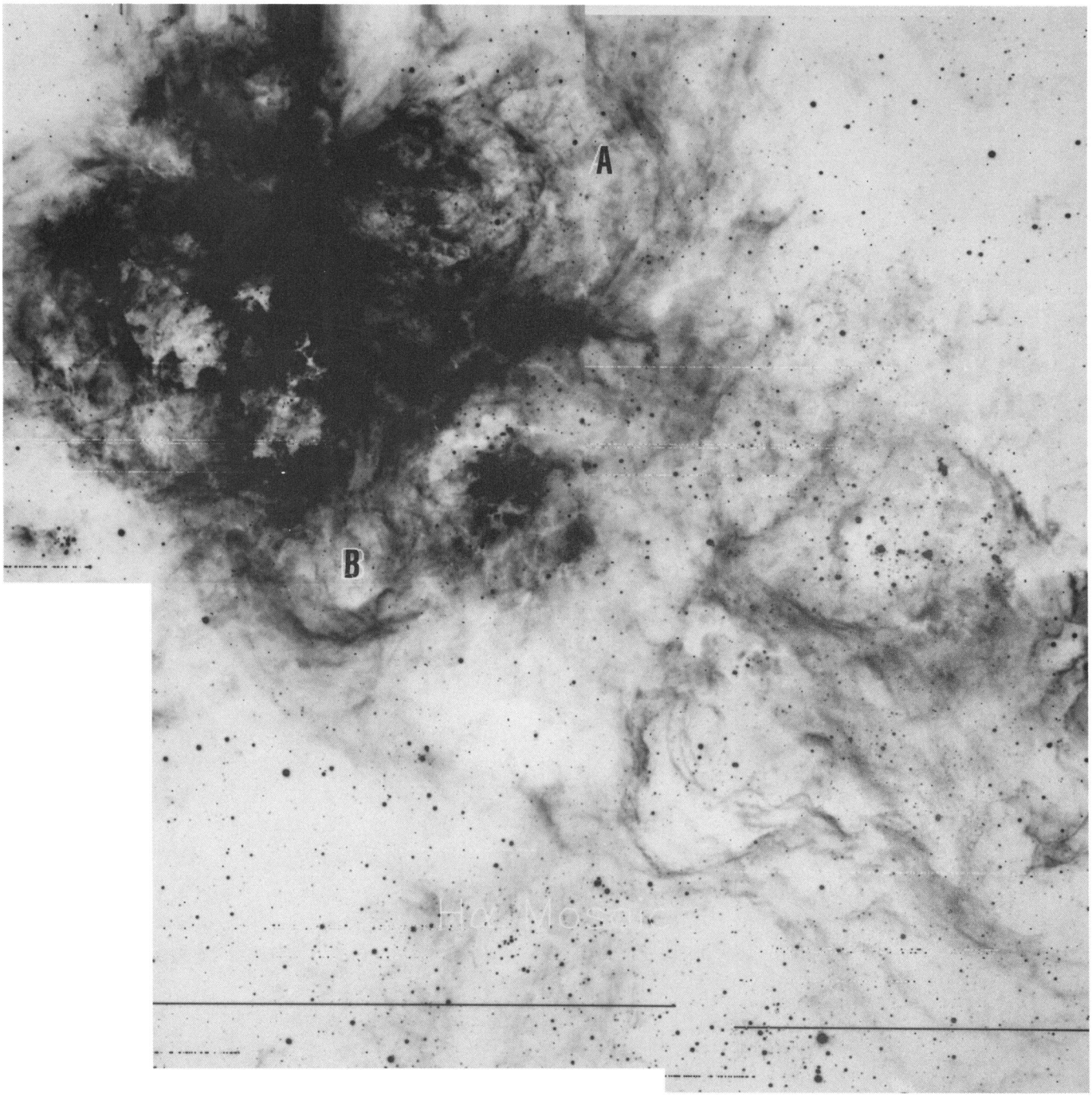

FIG. 3.—Hα 30′ × 30′ mosaicked CCD image of the 30 Doradus field, with positions of the double shock fronts (A) and the large-scale windblown bubble (B) marked.

CHENG et al. (see 395, L31)

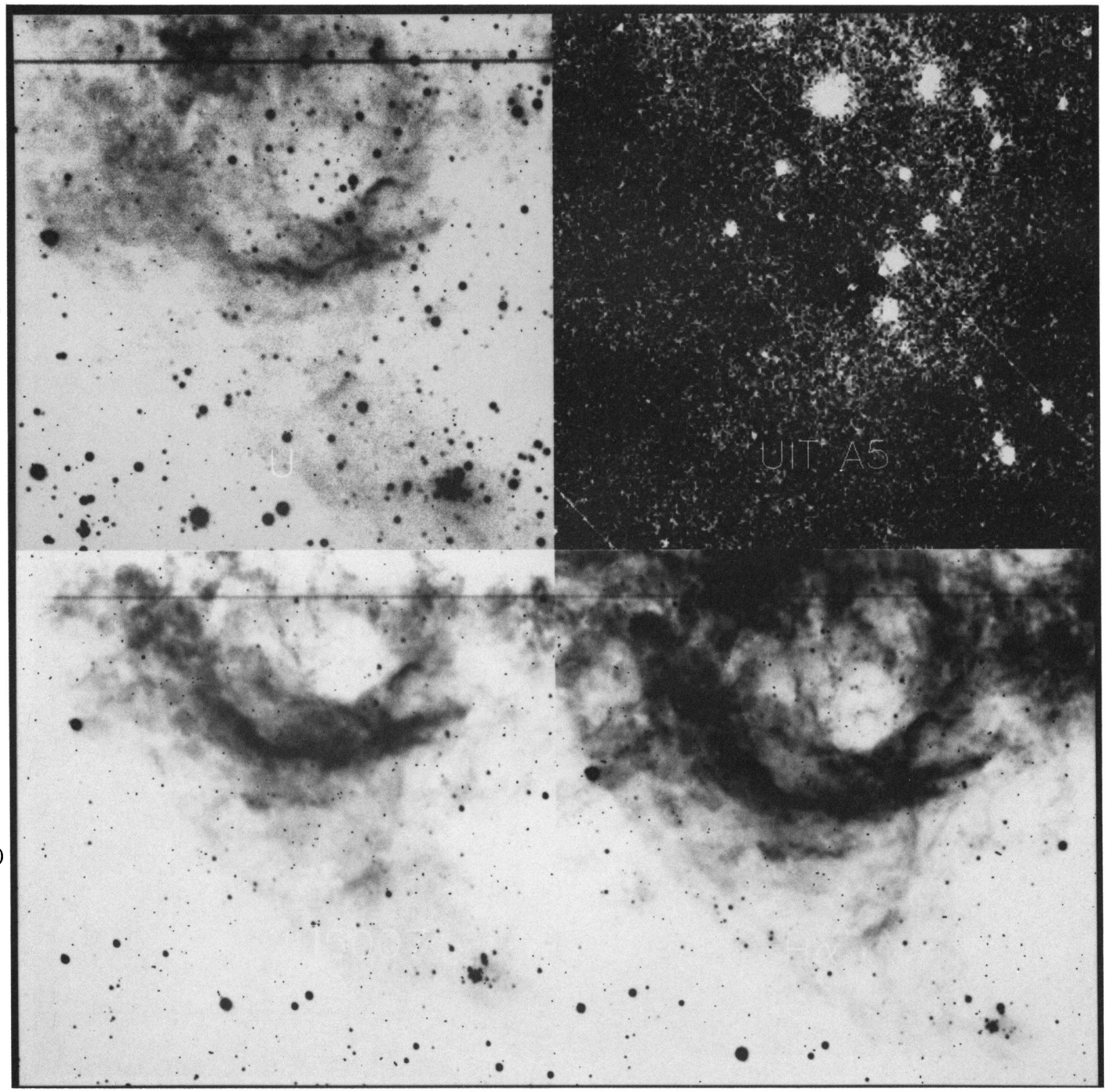

FIG. 4.—Images of the ~60 pc diameter windblown bubble 7′ south of the 30 Doradus center, as marked in Fig. 3, position B. (*a*) *U*; (*b*) [O III] λ5007; (*c*) UIT A5 (λ_0 = 2558 Å, FWHM + 456 Å, exposure time = 472 s); (*d*) Hα.

CHENG et al. (see 395, L31)

shell structure seen in the A5 (2558 Å) image. Another promising subject for study is the Bubble Nebula, N157C, located at $\sim 15'$ southwest of 30 Doradus. The optical image shows a large filamentary 6′ diameter loop with LH 90 in the center. Mathewson et al. (1985) have suggested that this nebula has been produced by both stellar winds and one or more SNRs within the bubble. The central OB association LH 90 (NGC 2044) contains several tight clusters of hot stars and is peculiarly rich in W-R stars. We find that the LH 90 cluster is a strong UV source, but is invisible in the IR (see Fig. 5 [Pl. L17]).

3.3. *The Dark Feature Extending through N157A, N157B, and N157C*

There are huge UV brightness variations over the 30 Doradus and SN 1987A regions. Among the faint UV emission areas, some are simply UV light reflected from the dust. The large-scale distribution of dust can be identified unambiguously using the UV and IR observations. We find an extended diffuse UV structure at low flux levels in the 30 Doradus region running through its three major components, N157A, N157B, and N157C. A similar large-scale structure is also evident in the *IRAS* 60 μm HiRes image of this region. In Figure 5 the 60 μm contours centered on N157A exhibit a prominent component elongated $\sim 27'$ along the axis of the diffuse UV feature. The coincident extended UV feature is apparently due to forward scattering by dust grains. The combined UV, optical, and IR data enable us to study the stellar content and dust morphology in this region.

4. SUMMARY

In this *Letter* we report a preliminary analysis of UIT images in the 30 Doradus region. We have obtained photometry for the 30 Doradus cluster and its UV-bright core, R136, in various UIT bandpasses. We find that $\sim 14\%$ of the total far-UV light ($\lambda_0 = 1892$ Å) and $\sim 16\%$ of the total near-UV light ($\lambda_0 = 2558$ Å) of the 3′ diameter 30 Doradus cluster originates from the region within 5″ of R136. We have also measured the UV magnitudes and colors of R136 and other known O and Wolf-Rayet WN stars in the same field. The UIT data, combined with published observations at longer wavelengths, indicate that R136a1, the brightest component of R136, is not a supermassive star.

We have performed a qualitative comparison between the UIT images, *Einstein* X-ray data, *IRAS* HiRes images, and ground-based CCD images in [O III] λ5007, Hα, *B*, *R*, *U*, and Strömgren *u*. Several stellar windblown cavities and extended large-scale features have been identified which merit further study. The extended diffuse UV feature detected in the UIT images is correlated with the IR structure seen in the *IRAS* 60 μm HiRes image, which suggests the existence of large amounts of widely distributed dust in this region.

In this study we have used data retrieved from the SIMBAD data base of the Strasbourg, France, Astronomical Data Center. We would like to thank Fred Bruhweiler for useful discussions. We also thank J. Hill for providing instruction in using the UIT data reduction software.

REFERENCES

Cassinelli, J. P., Mathis, J. S., & Savage, B. D. 1981, Science, 212, 1497
Conti, P. S., & Burnichon, M. L. 1975, A&A, 38, 467
Fitzpatrick, E. L. 1985, ApJ, 299, 219
Forest, T. A., Spenny, D. L., & Johnson, R. W. 1988, PASP, 100, 683
Koornneef, J., & Mathis, J. S. 1981, ApJ, 245, 49
Ledoux, P. 1970, in Saas-Fée Course, La Structure interne des étoiles (Sauverny: Observatoire de Genève), 45
Lortet, M.-C., & Testor, G. 1991, A&AS, 89, 185
Maeder, A. 1980, A&A, 92, 101
Mathewson, D. S., Ford, V. L., Tuohy, I. R., Mills, B. Y., Turtle, A. J., & Helfand, D. J. 1985, ApJS, 58, 197
Melnick, A. P. J., Seggewiss, A., & Shara, M. M. 1985, ApJ, 295, 109
Schmidt-Kaler, Th. 1980, Trans. IAU, 17B, 208
Schmidt-Kaler, Th. 1980, Trans. IAU, 17B, 208
Seggewiss, W. 1984, in IAU Symp. 108, Structure and Evolution of the Magellanic Clouds, ed. S. van den Bergh & K. S. de Boer (Dordrecht: Reidel), 266
Stecher, T. P., et al. 1992, ApJ, 395, L1
Walborn, N. R. 1986, in IAU Symp. 116, Luminous Stars and Associations in Galaxies, ed. C. W. H. de Loore, A. J. Willis, & P. Laskarides (Dordrecht: Reidel), 185
———. 1991, in IAU Symp. 148, The Magellanic Clouds and Their Dynamical Interaction with the Milky Way, ed. R. F. Haynes & D. K. Milne (Dordrecht: Kluwer), 145
Wang, Q., & Helfand, D. J. 1991, ApJ, 370, 541
Weigelt, G., et al. 1991, ApJ, 378, L21
Weigelt, G., & Baier, G. 1985, A&A, 150, L18

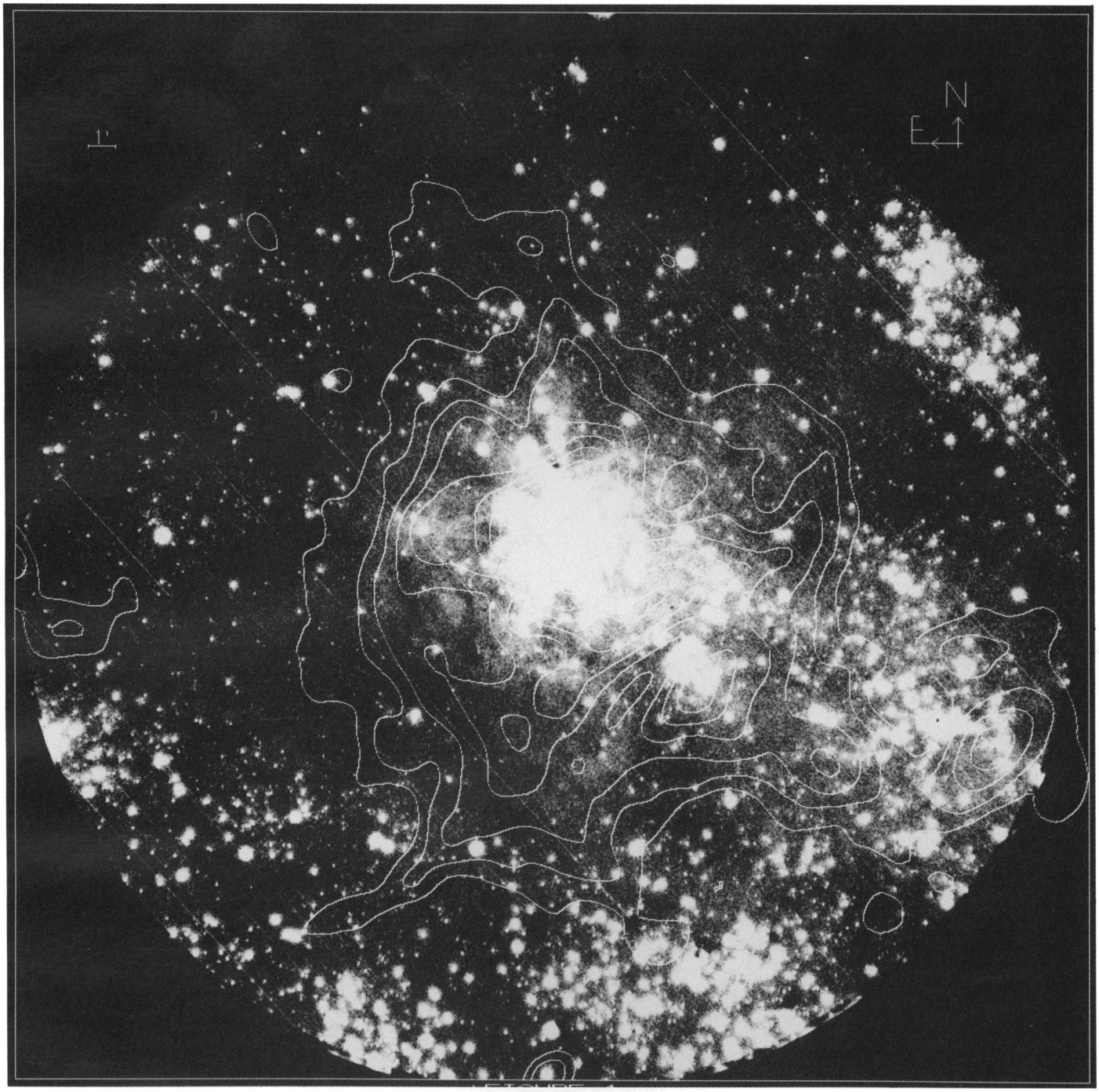

FIG. 5.—UIT near-UV image of the 30 Doradus field (A5, $\lambda_0 = 2558$ Å, FWHM = 456 Å, exposure time = 472 s, 40′ diameter) with the *IRAS* HiRes 60 μm contours overlaid.

CHENG et al. (see 395, L32)